



OPEN

Microbial communities and their roles in the Cenozoic sulfurous oil reservoirs in the Southwestern Qaidam Basin, Western China

Yue Jiao¹, Liyun An², Wei Wang³, Jian Ma¹, Chaodong Wu^{1✉} & Xiaolei Wu⁴

The latest discovery of sulfurous natural gas marked a breakthrough in the Cenozoic natural gas exploration in the southwestern margin of Qaidam Basin. The 16S rRNA analyses were performed on the crude oil samples from H₂S-rich reservoirs in the Yuejin, Shizigou and Huatugou profiles, to understand the sulfurous gas origin, which was also integrated with carbon and hydrogen isotopes of alkane and sulfur isotopes of H₂S collected from the Yingxiangling Area. Results show that the microorganisms in samples can survive in the hypersaline reservoirs, and can be classified into multiple phyla, including *Proteobacteria*, *Planctomycetes*, *Firmicutes*, *Bacteroidetes*, and *Haloanaerobiaeota*. Methanogens are abundant in all of the three profiles, while sulfate-reducing bacteria are abundant in Yuejin and Huatugou profiles, contributing to the methane and H₂S components in the natural gas. The carbon, hydrogen and sulfur isotopes of sulfurous natural gas in the Yingxiangling Area show that the natural gas is a mixture of coal-type gas and oil-type gas, which was primarily derived from thermal degradation, and natural gas from the Yuejin and Huatugou profiles also originated from biodegradation. The isotopic analysis agrees well with the 16S rRNA results, i.e., H₂S-rich natural gas from the Cenozoic reservoirs in the southwest margin of the Qaidam Basin was primarily of thermal genesis, with microbial genesis of secondary importance.

Hydrogen sulfide (H₂S) is one of the non-hydrocarbon gases commonly found in carbonate reservoirs. The acidity of abundant H₂S will cause corrosion and sulfide deposits in the pipelines during gas extractions^{1,2}, and the toxic H₂S may endanger the successful completion of the operation^{3,4}. Therefore it is of great challenge to develop deeply-buried carbonate reservoir under complex geological conditions, e.g., high temperature and pressure, high H₂S and CO₂ content^{5,6}, and it is essential to assess the concentration of H₂S before drilling⁷. The H₂S-rich gas resource in China is up to 1 × 10¹⁰ m³, which is widely distributed in large sedimentary basins with thick carbonate reservoirs, e.g., Bohai Bay Basin, Sichuan Basin, Tarim Basin and Ordos Basin^{8,9}. The current researches on sulfurous natural gas mainly focus on compositions and isotopes of sulfur compounds and H₂S origin^{6,10–12}. Three primary H₂S sources can be identified based on the burial depth and thermal maturity¹³: bacterial sulfate reduction (BSR), thermochemical sulfate reduction (TSR) and thermal decomposition reaction (TDR)^{14,15}. Also, a small amount of H₂S are derived from tectonic activities and volcanic eruptions, where H₂S is not stable during migration and preservation^{12,16}. The BSR is one of the main contributors to abundant H₂S in oil and gas reservoirs¹⁷, with organic matter and sulfate as reactants^{10,18}. BSR generally occurs in shallow-buried reservoirs with the participation of sulfate-reducing bacteria under low temperature (< 60 °C, with the peak at 20–40 °C), its effect on the gas generation in reservoirs is a research hotspot in recent years^{19,20}.

The Qaidam Basin is a huge petroliferous basin with an average elevation of ~ 3000 m (9800 ft) inside the Tibetan Plateau, northwest China^{21,22}. It can be structurally divided into the northern fault block, the western depression and the eastern depression. Huge natural gas resource potential has been discovered in the Qaidam Basin^{23,24}, including the Jurassic coal-type gas at the northern margin, the Paleogene-Neogene oil-type gas in the southwest, and the Triassic biogenetic gas in the Sanhu area^{25–28}. The natural gas in the southwest is mainly originated from four sources: oil-associated gas from sapropel-type kerogen (type I kerogen), mixed oil-associated gas, coal-type gas and mixed gas^{5,29}. Recently, the S58 well and SX58 well, high-sulfur gas producers, were

¹The Laboratory of Orogenic Belts and Crustal Evolution, School of Earth and Space Science, Peking University, Beijing 100871, China. ²College of Architecture and Environment, Sichuan University, Chengdu 610065, China. ³The No. 1 Oil Extraction Plant, Qinghai Oilfield Company, PetroChina, Haixi 817000, Qinghai, China. ⁴College of Engineering, Peking University, Beijing 100871, China. ✉email: cdwu@pku.edu.cn

discovered in the Yingzhong Area in the southwestern margin of the Qaidam Basin, with H_2S volume fractions of 1.74% and 2.75%, respectively, while reservoirs in the western Qaidam Basin were low in sulfur content³⁰. The western Qaidam Basin underwent an epeiric sea–continent transition from Paleozoic to Mesozoic^{31,32}, and was an anoxic and hypersaline semi-deep lake in the Paleogene, where developed a small-scale invasion with widely-distributed salinization deposits^{33–36}. Gypsum and source rocks are interbedded in the Lower Ganchai-gou Formation in the Yingxiongling Area^{37,38}, where sulfur isotopes are heavier than those of contemporaneous seawater due to hydrocarbon or sulfate reduction of microorganisms^{5,12}.

Oil reservoirs are commonly characterized by high temperature, high salinity, and high pressure, where microorganisms (including bacteria and archaea) are prevailing, e.g., denitrifiers, sulfate-reducing bacteria, methanogens^{39–42}. They take hydrocarbon, sulfur- and nitrogen-containing compounds in crude oil and deposits as energy sources with different survival strategies^{43,44}, e.g., using specific membrane or cell walls to avoid the migration of high-concentration salt, pumping out ions and adjusting the osmotic pressure of interior/external cells^{45,46}. Currently, the 16S rRNA sequencing technology allows for species level determination and improves the efficiency and accuracy of microbial community identification⁴⁷, and has been applied to analyze function and distribution of sulfate-reducing bacteria, hydrocarbon degradation bacteria, methanogens, ferment bacteria, etc.^{48–52}. In this study, the 16S rRNA sequencing and isotopic analysis were carried out on crude oil samples collected from Yuejin, Shizigou and Huatugou profiles in the southwestern margin of the Qaidam Basin, to (1) describe the metabolism pathways of microbial communities, (2) decipher the gas components and carbon, hydrogen, sulfur isotopic compositions of natural gas in the Yingxiongling Area, and (3) discuss the origination of sulfurous natural gas in southwestern Qaidam Basin.

Geological setting

The Qaidam Basin, a NWW-extending irregular triangle basin, is located in the north of the Qinghai-Tibet Plateau, which is bounded by the eastern margin of the Altun Mountains in the west and the southern margin of the Qilian Mountains in the east⁵³, Fig. 1). It is a typical Mesozoic-Cenozoic continental petroliferous sedimentary basin, with area and an average altitude of 12.1×10^4 km² and 2900 m, respectively^{54,55}. Large-scale strike-slip and rotation have occurred due to the activities of the Qinghai-Tibet Plateau since the Cenozoic⁵⁶, where the subsidence center has been shifted from west to east, developing an unified large subsidence center in the Sanhu

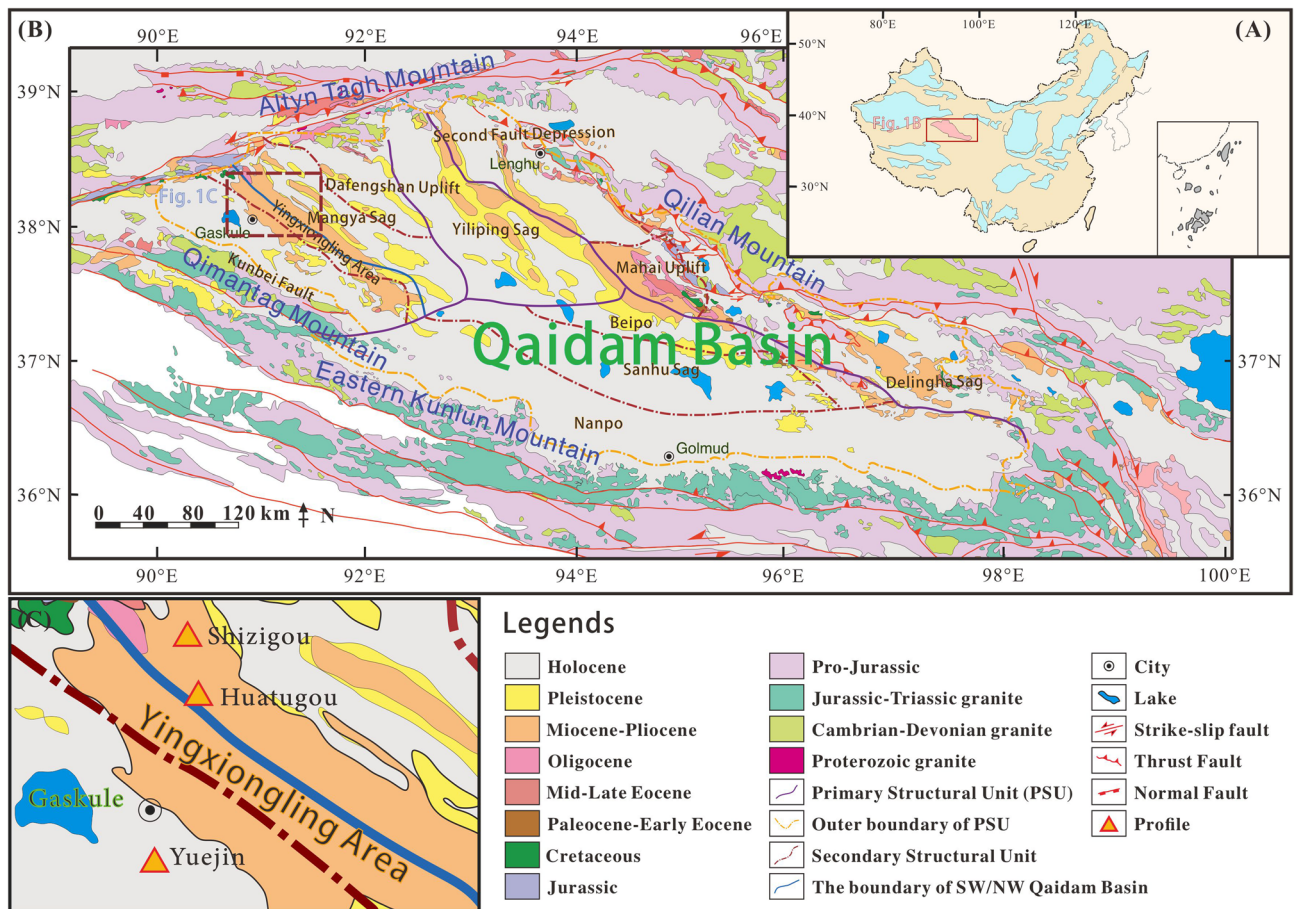


Figure 1. The geological map of the Qaidam Basin with sampling locations (A) The location of Qaidam Basin in China, modified after Zou et al.²², (B) Geological map of the Qaidam Basin, modified after Cheng et al.⁵³, (C) Sampling profiles in the southwestern Qaidam Basin.

area in the east during the Quaternary^{57,58}. Consequently, the Jurassic freshwater lacustrine source rocks were developed in the northern margin, the Paleogene-Neogene saline lacustrine source rocks were deposited in the western margin, and the Quaternary biogenic-gas source rocks were formed in the eastern margin⁵⁹.

The Paleogene and Neogene source rocks in the western Qaidam Basin are dominated by lacustrine dark mudstone and calcareous mudstone with gypsum and salt beds^{37,60}, the salinized deposits mainly originated from hot-arid climate with high evaporation³⁶, which is mainly oil-prone, and generates low-mature to mature oil with minor gas production^{61,62}. However, the proved natural gas reserves are currently far from the estimated geological natural gas resources, indicating potential gas exploration prospect^{30,63}. The Yingxiongling Area is located in the west part of Mangya Depression, which is characterized by well-deformed folds and major faults⁵⁴. The large-scale detachment faults connect the high-quality Paleogene source rocks with middle-shallow buried structural traps, while the middle-shallow faults possess good lateral plugging performance which are favorable for hydrocarbon preservation⁶⁴. A large number of oil reservoirs were developed in the Yingxiongling Area, including the Shizigou, Huatugou, Youshashan and Yingdong reservoirs⁶⁵. The structural pattern of the Yingxiongling Area varies significantly from west to east. It is characterized by a double-layer structure in vertical in the middle and the west, i.e., the upper layered salt rocks can work as a high-pressure cap rocks, and fractures and joints at the subsalt reservoirs are conducive to oil and gas migration, where CH₄ is mainly derived from crude-oil-associated gas^{62,66,67}. The eastern part of the Yingxiongling Area lacks salt caprocks (mainly halite) and possess a relatively simple structural pattern, with episodic charging of petroleum occurred from deep to shallow, in which natural gas is the by-product of condensate oil^{56,68}. Recently, oil reservoirs containing high levels of H₂S have been discovered in the middle of the Yingxiongling Area, this is different from the conventional reservoirs containing low sulfur content in former studies. Tian et al.¹² suggested that the H₂S in Yingxiongling Area is mainly derived by TSR, and the high temperature (approximately 181 °C) and burial depth (>4500 m) are not favorable for BSR, but the origin of H₂S still requires further discussion.

Samples and methods

Crude oil samples were taken from sulfurous oil reservoirs from the interval of Eocene to Neogene, in the Yuejin, Shizigou, and Huatugou profiles. The sampling profiles are shown in Fig. 1C, and the sample information are listed in Table 1. Most of the samples are heavy oil, while the sample H-2 from Huatugou profile is light oil with high level of H₂S. The 16S rRNA analysis were performed on these samples. The carbon, hydrogen and sulfur isotopic compositions of the sulfurous natural gas in Huatugou profile are tested.

16S rRNA analysis. To extract total microbial genomic DNA of crude oil, we added three volumes of isooctane (2,2,4-trimethylpentane), mixed thoroughly, and let it stand overnight at room temperature. The precipitates were obtained after centrifuged at 5000 × g for 30 min at 4 °C, washed, and re-suspended twice with three volumes of isooctane, then centrifuged at 5000 × g for 30 min at 4 °C. After dried in vacuum oven at 55 °C, for 2 h, the precipitates were collected for the total microbial genomic DNA extraction by using FastDNA® SPIN Kits for Soil (Axygen Biosciences, USA; MP Biomedicals, USA) following the procedures in accordance with the manufacturers' instructions. To be detailed, (i) Sodium Phosphate Buffer and MT Buffer were used to protect DNA during the cell-wall-breaking by lysozyme, (ii) Buffer G-B, DV, and BV were used to remove cell walls, lipids, and proteins, respectively; (iii) Buffer W1, W2 and Eluent were utilized to collect nucleic acid molecules.

Sequencing and data analysis. The V3—V4 region of bacterial 16S rRNA genes were amplified using 338F (ACT CCT ACG GGA GGC AGC AG) and 806R (GGA CTA CHV GGG TWT CTA AT) primers. The PCR products were purified and quantified, and then were sequenced on Illumina MiSeq platform as described previously⁶⁹. The acquired sequences were filtered for quality control as previously described⁷⁰. To achieve what, all chimeric sequences were removed using the USEARCH tool based on the UCHIME algorithm 2.3. Sequences were then split into operational taxonomic units (OTUs) based on a threshold of 97% identity between nucleotide sequences using the UPARSE pipeline^{71–73}. In addition, OTUs with fewer than two sequences were removed. Each bacterial OTU representative sequence was assigned taxonomy against the Silva database (release 128⁷⁴). OTUs annotated to bacterial domain were retained, and OTU tables were resampled to a minimum number of sequences.

No	Profile	Well	Interval	Depth/m	Note
Y-1	Yuejin	Yueqian 1-71-21	the Lower N ₁	2575–2599	Heavy oil
Y-2	Yuejin	Yue 17–28	the E ₃ ¹	3279–3475	Heavy oil
Y-3	Yuejin	Yueqian 1-49-1	the Lower N ₁	2450–2550	Heavy oil
S-1	Shizigou	Shixin 41H4-3-510	the E ₃ ²	4142–4839	Heavy oil
S-2	Shizigou	Shi41H-1-1-506	the E ₃ ²	4384–5133.5	Heavy oil
H-1	Huatugou	N13-6-5	the E ₃ ²	1479–1621	Heavy oil
H-2	Huatugou	SX58	the E ₃ ²	5502–5514	Light oil, high H ₂ S

Table 1. Information of sulfurous crude oil sampled from the southwest of the Qaidam Basin.

Natural gas isotope measurement. The H₂S-rich natural gas was collected from the Well SX58 in the Huatugou profile in the southwest of Qaidam Basin. The H₂S in natural gas was solidified with cadmium acetate solution (25 g cadmium acetate solid was dissolved in 3.5 mol/L HAC per liter) to generate yellow cadmium sulfide precipitate based on the sulfur component separation method⁷⁵. After that, black silver sulfide precipitates were produced by adding 0.05 mol/L silver nitrate solution and was washed with distilled water. The sulfur isotope analysis was completed at the Chinese Academy of Geological Sciences. The carbon and hydrogen isotope tests of natural gas were conducted at the China Petroleum Exploration and Development Research Institute. Experiment details can be referred from previous studies⁷⁶.

Results and discussion

Abundance of different microbial communities. A total of 1338 OTUs were identified via the 16S rRNA sequencing from seven samples in the three profiles in southwestern Qaidam Basin. After abundance normalization, top 15 Phyla, including *Proteobacteria*, *Planctomycetes*, *Firmicutes*, *Bacteroides*, and *Haloanaerobes*, were identified with abundance variations shown in Table S1 and Fig. 2. The top 32 OTUs, with abundance accounting for about 80% of the total value, were selected for the next analysis. These bacteria typically thrive depending on hydrocarbons^{77–80}, nitrogenous compound⁸¹, and sulfur compound⁸², and can survive in the hypersaline and alkaline environment^{83–86}. Their specific abundance, scientific name and metabolic behaviors are listed in Table S2. Among them, methanogens, sulfate-reducing bacteria and nitrate-reducing bacteria, which are widely spread in global oil reservoirs^{87–89}, were unevenly distributed in the crude oil samples from the southwestern Qaidam Basin (Fig. 3).

Methanogens. Among the top 32 OTUs, eleven of them are involved in methane metabolism, which can be divided into three categories: methanogen (I), synergistically methanogenesis (II) and methylotrophic bacteria (III). They are unevenly distributed in the Yuejin, Shizigou and Huatugou profiles (Fig. 3A). The type I is methanogen, including OTU_11 and OTU_12, which can be classified into *Actinobacteria* and *Chloroflexi*, respectively. They are frequently observed at high-temperature oil reservoirs^{90,91} and can degrade long-chain n-alkanes into methane^{92,93}. The OTU_11 abundance is high in the Yuejin and Shizigou profiles (1.15–2.8%), while the OTU_12 abundance is high in the Huatugou profile (up to 4.29%), whose occurrence might contribute positively to methane generation at reservoirs in the southwestern Qaidam Basin. The type II, OTU_22 and OTU_30 of the genus *Bacillus*, can produce surfactants to promote the formation of methane hydrate and enhance methane migration⁹⁴, with thermostability and salt-tolerance⁹⁵. Surfactants derived from OTU_31 and OTU_32 of the genus *Pseudomonas* can emulsify aliphatic compounds and aromatic hydrocarbons and cooperate with primary producers to promote methanogenesis⁹⁶. These bacteria abundance are high in samples Y-3, S-1, and S-2, indicating that the methane migration associated with microbial community also enhanced methane enrichment in Yuejin and Shizigou profiles. Different from that, OTU_3, OTU_13, OTU_16, OTU_21, and OTU_24 can use hydrocarbons, e.g., methane, and carbohydrate, as carbon sources for heterotrophy or autotrophy, consuming methane in the environment^{97–101}. All these bacteria are observed from three profiles, but are unevenly distributed in space. The OTU_3, OTU_13 and OTU_24 are relatively rich in the Yuejin and Shizigou profiles, while OTU_16 and OTU_21 possess high abundance in the Huatugou profile, confirming sufficient methane supply in these three profiles with different microbial communities.

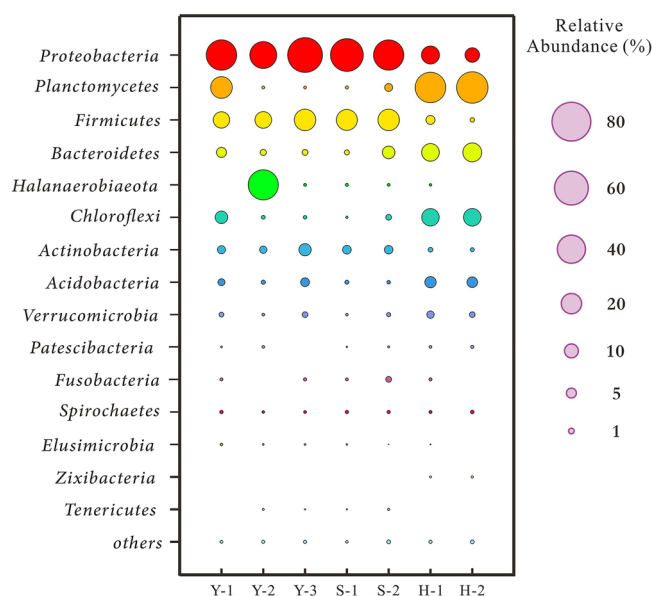


Figure 2. Bubble diagram of top 15 Phyla in samples from the Yuejin, Shizigou and Huatugou profiles.

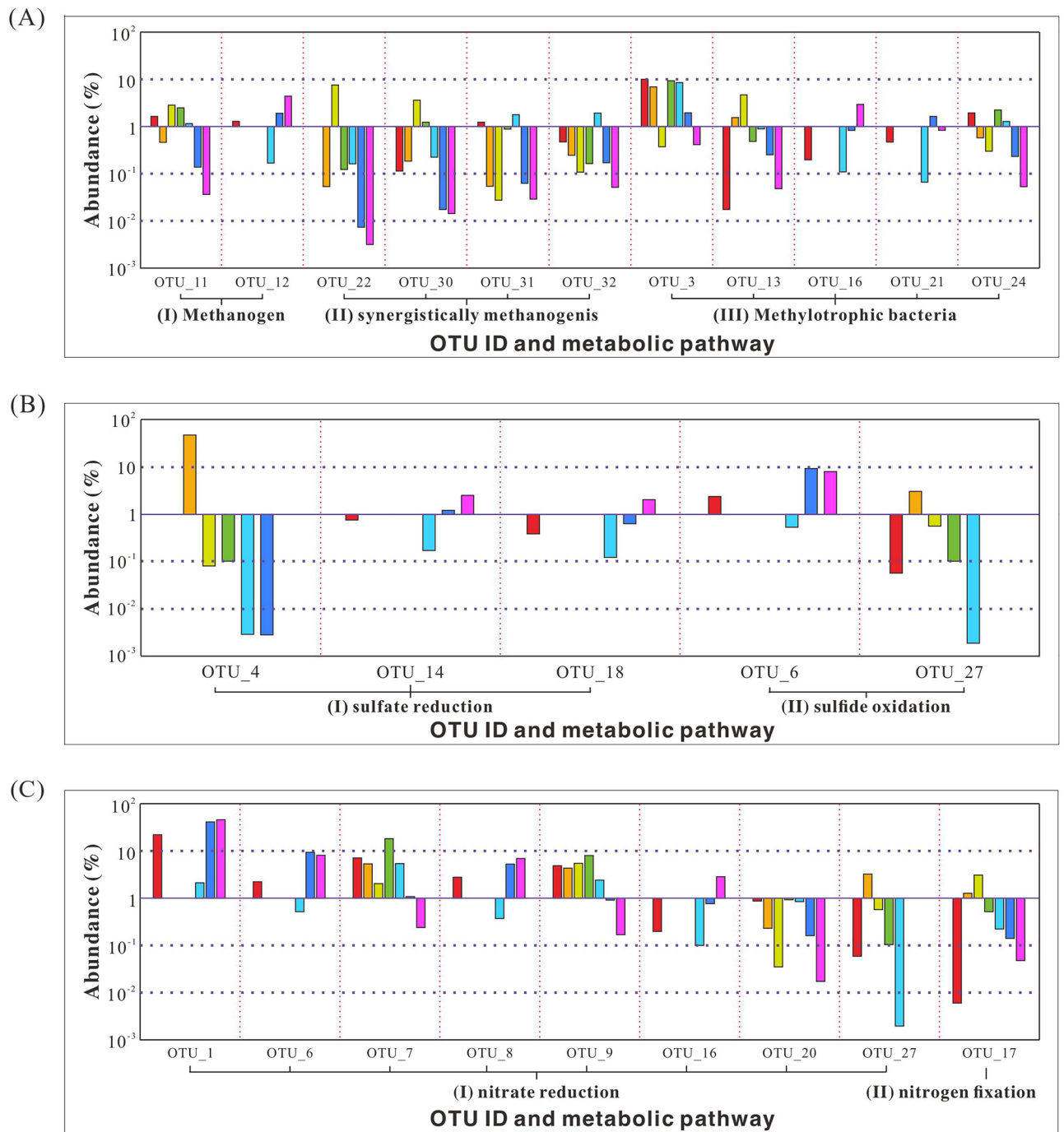


Figure 3. Histogram of microbial abundance involved in methane, sulfate and nitrate metabolism in the Yuejin, Shizigou and Huatugou profiles.

Sulfate-reducing bacteria. Five OTUs are involved in the metabolism of sulfur compounds, including sulfate reduction (I) and sulfide oxidation (II), respectively. They also unevenly distributed in the Yuejin, Shizigou, and Huatugou profiles (Fig. 3B). The type I includes OTU_4, OTU_14, and OTU_18, and can be classified into three phyla: *Halanaerobiaeota*, *Proteobacteria*, and *Bacteroidetes*. They can survive in saline-alkaline soil and hot spring with the temperature range of 4–92 °C and the pH range of 2.3–10.6^{102,103}, taking organic matter as the electronic donor to reduce sulfate, sulfite or thiosulfate to sulfide^{82,104}. The abundance of OTU_4 is extremely high in the sample Y-2 from the Yuejin profile (up to 47.37%), while OTU_14 and OTU_18 abundance are high in the sample H-2 from the Huatugou profile (2.57% and 2.12%, respectively). The OTU_14 can conduct anaerobic oxidation of methane (AOM) with methanogens, producing H₂S and decreasing CH₄ content¹⁰⁵. It agrees

well with the high H₂S content of the sample H-2 and is responsible for the H₂S occurrence at the sulfurous reservoirs in the Yuejin and Huatugou profiles. The type II bacteria, including OTU_6 and OTU_27, are sulfide-oxidizing nitrate-reducing bacteria (soNRB), can oxidize sulfide into sulfur or sulfate based on the proportion between nitrate and sulfide in reservoirs¹⁰⁶. The OTU_6, belonging to the genus *Bacteroides*, can take H₂S as the electron donor for denitrification reaction and oxidize H₂S to sulfur and further generates sulfate¹⁰⁷. The OTU_6 can be detected in three profiles, and is abundant in two samples from Huatugou profile, with relative abundance of 9.4% and 8.24%, respectively. The OTU_27, belonging to the genus *Comamonas*, can transform sulfide in the environment into sulfur¹⁰⁸, with abundance of 3.28% in the Y-2 sample, but was not detected from samples in the Huatugou profile. Sulfate minerals (e.g., celestite, barite, gypsum, and mirabilite) and sulfides (e.g., framboid pyrite), which regionally enriched in the Paleogene in the Yingxiongling Area^{36,109}, not only provided substrates for bacterial sulfate-reduction reaction, but also resulted in difference in sulfate-reducing bacteria abundance and sulfide-oxidizing bacteria abundance among the Yuejin, Shizigou, and Huatugou profiles.

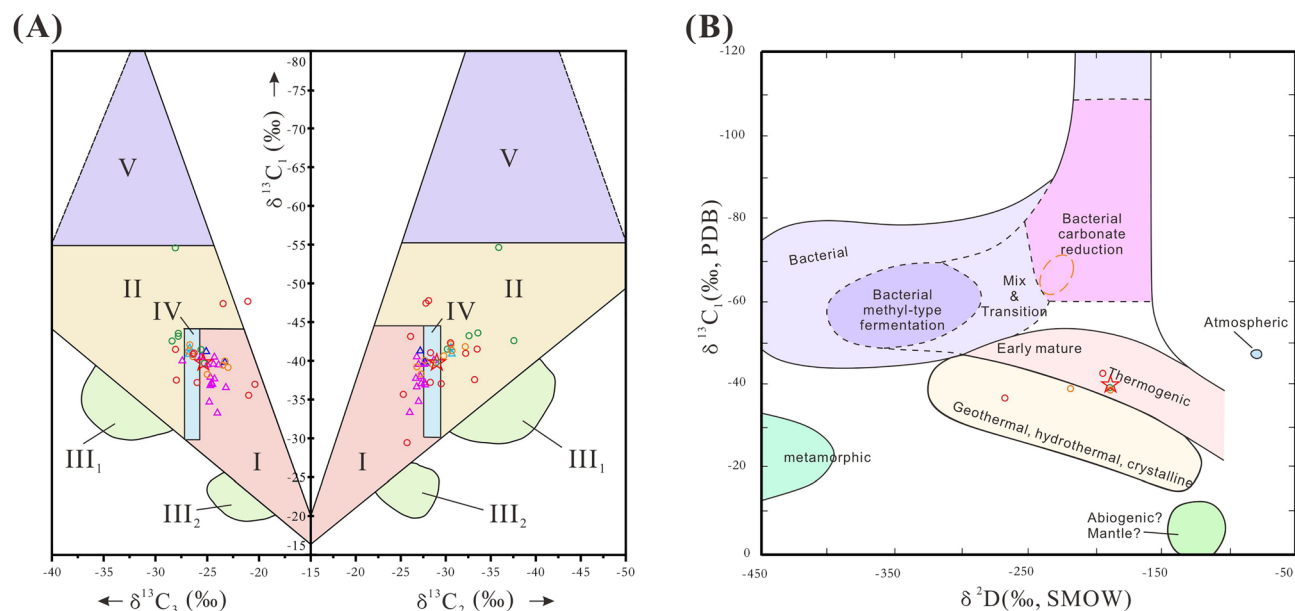
Nitrate-reducing bacteria. Nine OTUs are involved in the metabolism of nitrogen-containing compounds, including nitrate reduction (I) and nitrogen fixation (II), respectively, whose abundance was different in the Yuejin, Shizigou, and Huatugou profiles (Fig. 3C). The type I is nitrate-reducing bacteria (NRB), including OTU_1, OTU_6, OTU_7, OTU_8, OTU_9, OTU_16, OTU_20 and OTU_27, which can trap electrons from organic carbon (e.g., methane, amino acid, carboxylic acid, aromatic hydrocarbon^{110–112}), and reduce nitrate following an order: NO₂⁻ → NO → N₂O → N₂ → NH₄⁺^{113,114}. These microorganisms are abundant in the Yuejin profile, and show different abundance in Huatugou and Shizigou profiles. Specifically, the abundance of OTU_1, OTU_6, OTU_8 and OTU_16, are high in the Huatugou profile, while the abundance of OTU_7, OTU_9, OTU_20 and OTU_27 are high in the Shizigou profile. Furthermore, although OTU_6 and OTU_16 belong to NRB, they can use H₂S and CH₄ as electron donors to generate sulfate and CO₂, respectively^{97,107}, the enrichment of these bacteria confirmed the sufficient supply of H₂S and CH₄ in the Huatugou profile. The OTU_17 belongs to the nitrogen-fixing bacteria (type II), and can transform nitrogen into nitrate¹¹⁵, it is ecologically balanced with various nitrate reducing bacteria, and unevenly distributed at these three profiles.

Summarily, microbial communities with different metabolic behaviors are separated from crude oil samples in the Yuejin, Shizigou and Huatugou profiles, while methanogens, sulfate-reducing bacteria and nitrate-reducing bacteria abundance varied greatly among different profiles. These microorganisms can survive in high-temperature and hypersaline reservoirs, react with hydrocarbon, sulfate and nitrate to generate methane, H₂S and various nitrogenous compounds, respectively, indicating that microorganisms contributed greatly to the Cenozoic H₂S-rich natural gas in the southwestern margin of the Qaidam Basin.

Isotope distribution pattern of natural gas. The carbon, hydrogen and sulfur isotopic tests were conducted on the sulfurous natural gas from Well SX58 in Huatugou profile, and are compared with the collected data in the Yingxiongling Area from references. The hydrocarbon compositions of natural gas from the Huatugou profile is about 93.4%, which is dominated by methane with a proportion of 85.9% (Table S3). In general, natural gas reservoirs are commonly dominated by alkanes (e.g., methane, ethane and propane¹¹⁶), and the compound-specific carbon isotope and hydrogen isotope of natural gas can provide significant insight into the alkane sources^{117,118}. The carbon isotopes of methane, ethane, propane, butane and n-pentane in the tested sample increased successively with carbon number, which are -39.730‰, -28.915‰, -25.288‰, -24.715‰, and -24.652‰, respectively. The hydrogen isotopes of methane and ethane are -189.586‰ and -141.185‰, respectively. The non-hydrocarbon component in natural gas accounts for about 5.6% and is dominated by H₂S (with a proportion of 2.8%, and sulfur isotope of 32.2‰). This is close to the H₂S content (2.75%) and sulfur isotope value (32.5‰) in the middle Yingxiongling Area⁵.

Generally, organic gas can be characterized by the increasing carbon isotope (δ¹³C) of alkanes with carbon numbers, while alkanes from inorganic gas, fractured carbonate rocks, tight reservoirs and coal gas present reversals in carbon isotopes^{13,119}. Natural gas or carbonate generated by microbial reaction is generally low in ¹³C, because light isotope can be preferentially utilized by microorganisms¹²⁰. The carbon isotopic values of methane, ethane and propane in the southwestern margin of the Qaidam Basin are in ranges of -54.6‰ to -29.4‰, -37.6‰ to -25.4‰, -28.4‰ to -13.1‰, respectively (Table S3^{121–124}), which are defined as oil-type gas, coal-type gas and mixed gas, with no carbon isotopic reversals (Fig. 4A¹²⁵).

Five samples (Table S3) with δ¹³C₁ < -45.5‰ were found in the Yuejin and Huatugou profiles by Chen et al.⁷⁶, Liu et al.¹²⁶ and Li et al.¹²⁷. The lowest value was about -54.6‰ and was close to the value of biogenic gas (-55‰) proposed by Ni et al.¹²⁸. Biomarker analysis by Chen et al.⁷⁶ confirmed that light hydrocarbons in some samples from the Yuejin and Huatugou profiles were derived from the degradation of crude oil by microorganism. It agrees well with the above analysis of microbial community in section "Abundance of different microbial communities". Furthermore, the hydrogen isotopes of methane in natural gas can be used to identify the natural gas origin. Deuterium isotope is gradually enriched with increasing maturity of natural gas, where δD of organic gas can be characterized by a positive sequence trend, which is similar to the carbon isotope distribution. Hence, the crossplot of δD and δ¹³C can distinguish the origin of methane^{129,132}. Among the collected isotope data, few samples were performed with carbon and hydrogen isotopes at the same time, where the δD of methane was between -267‰ and -189‰. The measured δD of the sulfurous natural gas is -189.586‰ (Fig. 4B). Combined with above carbon isotope values (-54.6‰ to -29.4‰), it can be confirmed that the natural gas was mainly derived from thermal degradation, at low-maturity stage to maturity stage. Compared with intensive negative ¹³C₁ shifts in the Quaternary biogenic gas in the eastern Qaidam Basin (-72.3 to -60.53‰^{126,130,131}), few samples from the Yingxiongling Area in the southwest of Qaidam Basin present minor negative drifts. Therefore, the H₂S-rich



Legends

- | | | |
|--|--|--|
| I Coal-derived gas | II Oil-associated gas | III Mixed gas with carbon isotopic reversal |
| IV Coal-derived gas and/or oil-associated gas | V Biogenic gas | |
| ○ Yuejin | ○ Shizigou | ○ Huatugou |
| △ Yingxi | △ Yingzhong | △ Yingdong |
| ★ Natural gas containing H ₂ S in Huatugou profile (this study) | | |

Figure 4. Carbon and hydrogen isotopes of natural gas in the Yingxiongling Area, southwestern Qaidam Basin. (A) carbon isotopes; (B) hydrogen isotopes, modified after Feng et al.¹²⁵.

natural gas in the southwest of Qaidam Basin was derived from both thermal degradation and biodegradation, with the former of the most importance.

Biogenic gas is generally derived from biological fermentation and biological reduction¹³². Compared with sulfate (the reactant), the preferential use of light isotopes by microorganisms can bring a negative shift of 15–25‰ to sulfur isotopes in the H₂S of BSR origin^{133,134}. The TSR requires sufficient sulfate supply and high temperature, where sulfur isotopes in the H₂S do not drift greatly, usually between 5‰ and 15‰^{8,16,135}. The isotopic data of H₂S in the southwestern margin of the Qaidam Basin was poorly reported in previous studies. The tested sulfur isotope of H₂S-rich natural gas in this paper is 32.2‰, which does not present significant fractionation compared with the sulfur isotopes (30.3–33.5‰) of equivalent sulfate minerals (e.g., anhydrite, glauberite¹³⁶). Hence, the H₂S from the sulfurous oil reservoirs in the southwest of Qaidam Basin is primarily of thermal genesis¹², with microbial genesis of secondary importance.

The formation of H₂S is an ongoing process from the geological period to the present¹³⁷. The discussion on the H₂S origin is beneficial for oil & gas operators in the Qaidam Basin, because it will not only improve the theory of hydrocarbon generation in sulfurous reservoirs, but also help to better discover the high-sulfur intervals in exploration and development.

Conclusions

1. Microorganisms were extracted from crude oil samples from the Yuejin, Shizigou, and Huatugou profiles in the southwestern margin of the Qaidam Basin through integrating Axygen and MP FastDNA SPIN kits and were examined using 16S rRNA sequencing. Results show that the microorganisms vary greatly among these profiles, where methanogens and nitrate-reducing bacteria are well developed in the Yuejin, Shizigou, and Huatugou profiles, and sulfate-reducing bacteria are frequently observed in the Yuejin and Huatugou profiles. The spatial distribution of these microorganisms may be attributed to the different reservoir conditions, and contributed to the development of methane and H₂S in the sulfurous reservoirs.
2. The isotopic pattern of hydrocarbon components show no obvious reversals in carbon isotopes, indicating that the Cenozoic natural gas in the Yingxiongling Area is a mixture of coal-type gas and oil-type gas. It is believed that the natural gas was mainly derived from thermal degradation with microbial genesis of secondary importance, which can be confirmed by hydrogen isotope distribution. No obvious fractionation

occurred to sulfur isotopes of H₂S when compared with equivalent sulfate minerals, suggesting that the BSR was not the primary origin for H₂S in the sulfurous oil reservoirs.

Data availability

All data generated or analyzed during this study are included in this published article and its supplementary information files.

Received: 17 February 2023; Accepted: 21 April 2023

Published online: 17 May 2023

References

- Asadian, M., Sabzi, M. & Anijdan, S. H. M. The effect of temperature, CO₂, H₂S gases and the resultant iron carbonate and iron sulfide compounds on the sour corrosion behaviour of ASTM A-106 steel for pipeline transportation. *Int. J. Pres. Ves. Pip.* **171**, 184–193 (2019).
- Fu, Y. J., van Berk, W. & Schulz, H. Hydrogen sulfide formation, fate, and behavior in anhydrite-sealed carbonate gas reservoirs: A three-dimensional reactive mass transport modeling approach. *AAPG Bull.* **100**(5), 843–865 (2016).
- Cai, C. F. *et al.* Methane-dominated thermochemical sulphate reduction in the Triassic Feixianguan Formation East Sichuan Basin, China: Towards prediction of fatal H₂S concentrations. *Mar. Petrol. Geol.* **21**(10), 1265–1279 (2004).
- Yan, Z. F. *et al.* Preventing sour gas kicks during workover of natural gas wells from deep carbonate reservoirs with anti-hydrogen sulfide fuzzy-ball kill fluid. *Energy Sci. Eng.* **10**(8), 2674–2688 (2022).
- Tian, J. X. *et al.* Formation mechanism and distribution prediction of hydrogen sulfide in Yingxiangling area, Qaidam Basin. *Lithol. Reserv.* **32**(5), 84–92 (2020) (In Chinese).
- Zhu, G. Y. *et al.* Genesis and distribution of hydrogen sulfide in deep heavy oil of the Halahatang area in the Tarim Basin, China. *J. Nat. Gas Geosci.* **2**(1), 57–71 (2017).
- Wang, G. W., Hao, F., Zou, H. Y. & Li, P. P. Causes of variation in the concentration and distribution of H₂S in carbonate reservoirs of the Feixianguan Formation, Lower Triassic in the eastern Sichuan Basin. *Geoenerg. Sci. Eng.* **221**, 211381 (2023).
- Cai, C. F. *et al.* Sulfur and carbon isotopic compositions of the Permian to Triassic TSR and non-TSR altered solid bitumen and its parent source rock in NE Sichuan Basin. *Org. Geochem.* **105**, 1–12 (2017).
- Huang, L. M. New progresses in safe, clean and efficient development technologies for high-sulfur gas reservoirs. *Nat. Gas Ind. B* **2**(4), 360–367 (2015).
- Cai, C. F., Li, H. X., Li, K. K. & Wang, D. W. Thermochemical sulfate reduction in sedimentary basins and beyond: A review. *Chem. Geol.* **607**, 121018 (2022).
- Liu, W. H. *et al.* An isotope study of the accumulation mechanisms of high-sulfur gas from the Sichuan Basin, southwestern China. *Sci. China Earth Sci.* **59**, 2142–2154 (2016).
- Tian, J. X. *et al.* Genesis of hydrogen sulfide in natural gas reservoirs in the Western Qaidam Basin. *Interpretation* **9**(1), T223–T233 (2021).
- Milkov, A. V., Faiz, M. & Etiope, G. Geochemistry of shale gases from around the world: Composition, origins, isotope reversals and rollovers, and implications for the exploration of shale plays. *Org. Geochem.* **143**, 103997 (2020).
- Etiope, G. *et al.* Methane and hydrogen sulfide seepage in the northwest Peloponnesus petroliferous basin (Greece): Origin and geohazard. *AAPG Bull.* **90**(5), 701–713 (2006).
- Morad, D. *et al.* Limited thermochemical sulfate reduction in hot, anhydritic, sour gas carbonate reservoirs: The Upper Jurassic Arab Formation, United Arab Emirates. *Mar. Petrol. Geol.* **106**, 30–41 (2019).
- Zhu, G. Y. *et al.* TSR, deep oil cracking and exploration potential in the Hetianhe gas field, Tarim Basin, China. *Fuel* **236**, 1078–1092 (2019).
- Hao, F. *et al.* Evidence for multiple stages of oil cracking and thermochemical sulfate reduction in the Puguang gas field, Sichuan Basin, China. *AAPG Bull.* **92**(5), 611–637 (2008).
- Zhang, S. C. *et al.* Biogeochemical identification of the Quaternary biogenic gas source rock in the Sanhu Depression, Qaidam Basin. *Org. Geochem.* **73**, 101–108 (2014).
- Bhattarai, S., Cassarini, C. & Lens, P. N. L. Physiology and distribution of Archaeal methanotrophs that couple anaerobic oxidation of methane with sulfate reduction. *Microbiol. Mol. Biol. Rev.* **83**(3), e00074–e118 (2019).
- Liu, M. J., Deng, Q. G., Zhao, F. J. & Liu, Y. W. Origin of hydrogen sulfide in coal seams in China. *Safety Sci.* **50**(4), 668–673 (2012).
- Wu, L. *et al.* Cenozoic fault systems in southwest Qaidam Basin, northeastern Tibetan Plateau: Geometry, temporal development, and significance for hydrocarbon accumulation. *AAPG Bull.* **98**(6), 1213–1234 (2014).
- Zou, C. N. *et al.* Formation and distribution of volcanic hydrocarbons reservoirs in sedimentary basins of China. *Pet. Explor. Dev.* **35**(3), 257–271 (2008).
- Guo, Y. C., Cao, J., Liu, R. Q., Wang, H. F. & Zhang, H. Y. Hydrocarbon accumulation and alteration of the Upper Carboniferous Keluke Formation in the eastern Qaidam Basin: Insights from fluid inclusion and basin modeling. *J. Pet. Sci. Eng.* **211**, 110116 (2022).
- He, W. G., Barzgar, E., Feng, W. P. & Huang, L. Reservoirs patterns and key controlling factors of the Lenghu oil & gas field in the Qaidam Basin, northwestern China. *J. Earth Sci.-China.* **32**, 1011–1021 (2021).
- Chen, Z. & Zhang, C. S. The characteristics and hydrocarbon-generation model of Paleogene-Neogene System saline lacustrine facies source rocks in the Western Qaidam Basin, China. *J. Pet. Explor. Prod. Technol.* **9**, 2441–2447 (2019b).
- Guo, T. X. *et al.* Accumulation conditions and prospective areas of shale gas in the Middle Jurassic Dameigou Formation, northern Qaidam Basin, Northwest China. *Geol. J.* **53**(6), 2944–2954 (2018b).
- Shao, Z. Y. *et al.* Dynamic accumulation of the Quaternary shale biogas in Sanhu Area of the Qaidam Basin, China. *Energies* **15**(13), 4593 (2022).
- Wang, Y. Q. *et al.* Controls on the occurrence of beach-bar sandstone in a Neogene saline lake basin, southwestern Qaidam Basin, China. *Geol. J.* **57**(9), 3478–3495 (2022).
- Zeng, X. *et al.* Characteristics of Jurassic source rocks and oil and gas exploration direction in the piedmont zone between the southwestern Qaidam Basin and Altun Mountain. *Geol. J.* **57**(10), 4152–4166 (2022).
- Tian, J. X. *et al.* Geochemical characteristics and factors controlling natural gas accumulation in the northern margin of the Qaidam Basin. *J. Pet. Sci. Eng.* **160**, 219–228 (2018).
- Li, B. *et al.* Pre-cenozoic evolution of the northern Qilian Orogen from zircon geochronology: Framework for early growth of the northern Tibetan Plateau. *Palaeogeogr. Palaeoclimatol. Palaeoecol.* **562**, 110091 (2021a).
- Li, H. R., Qian, Y., Su, F. Y. & Wang, Y. Z. Paleozoic to Mesozoic magmatism in North Qaidam, Qinghai Province, NW China: Implications for tectonic evolution. *Gondwana Res.* **115**, 37–56 (2023a).

33. Chen, Q. L. *et al.* Geochemical characteristics of carbonate rocks in a salinized lacustrine basin: A case study from Oligocene formation in the Qaidam Basin, northwestern China. *Carbonate Evaporite* **35**(2), 40 (2020c).
34. Guo, P. *et al.* Paleosalinity evolution of the Paleogene perennial Qaidam lake on the *Tibetan Plateau*: Climatic vs. Tectonic Control. *Int. J. Earth Sci.* **107**, 1641–1656 (2018a).
35. Ma, J. *et al.* Biomarkers reveal Eocene marine incursions into the Qaidam Basin, north Tibetan Plateau. *Org. Geochem.* **166**, 104380 (2022).
36. Wang, J. G. *et al.* Sedimentary characteristics and genesis of the salt lake with the upper member of the Lower Ganchaigou formation from Yingxi Sag, Qaidam basin. *Mar. Petrol. Geol.* **111**, 135–155 (2020).
37. Yang, L. L. *et al.* Effects of gypsum-salt rock on mineral transformations in a saline lacustrine basin: Significance to reservoir development. *J. Pet. Sci. Eng.* **211**, 110240 (2022).
38. Yi, D. H. *et al.* Evolution characteristic of gypsum-salt rocks of the upper member of Oligocene Lower Ganchaigou Fm in the Shizigou area, western Qaidam Basin. *Nat. Gas Ind. B* **4**(5), 390–398 (2017).
39. Nazina, T. N. *et al.* Functional and phylogenetic microbial diversity in formation waters of a low-temperature carbonate petroleum reservoir. *Int. Biodeter. Biodegr.* **81**, 71–81 (2013).
40. Pannekens, M., Kroll, L., Müller, H., Mbow, F. T. & Meckenstock, R. U. Oil reservoirs, an exceptional habitat for microorganisms. *New Biotechnol.* **49**, 1–9 (2019).
41. Semenova, E. M., Ershov, A. P., Sokolova, DSh., Tourova, T. P. & Nazina, T. N. Diversity and biotechnological potential of nitrate-reducing bacteria from heavy-oil reservoirs (Russia). *Microbiology* **89**, 685–696 (2020).
42. Veshareh, M. J. *et al.* Nitrite is a more efficient inhibitor of microbial sulfate reduction in oil reservoirs compared to nitrate and perchlorate: A laboratory and field-scale simulation study. *Int. Biodeter. Biodegr.* **157**, 105154 (2021).
43. Oelgeschläger, E. & Rother, M. Carbon monoxide-dependent energy metabolism in anaerobic bacteria and archaea. *Arch. Microbiol.* **190**, 257–269 (2008).
44. Schwab, L. *et al.* Structural analysis of microbiomes from salt caverns used for underground gas storage. *Int. J. Hydrog. Energ.* **47**(47), 20684–20694 (2022).
45. Oren, A. *Salinibacter*, an extremely halophilic bacterium with archaeal properties. *FEMS Microbiol. Lett.* **342**(1), 1–9 (2013).
46. Ventosa, A., Nieto, J. J. & Oren, A. Biology of moderately halophilic aerobic bacteria. *Microbiol. Mol. Biol. Rev.* **62**(2), 504–544 (1998).
47. Numberger, D. *et al.* Characterization of bacterial communities in wastewater with enhanced taxonomic resolution by full-length 16S rRNA sequencing. *Sci. Rep.* **9**(1), 9673 (2019).
48. Grouzdev, D. S. *et al.* Genome sequences of green- and brown-colored strains of *Chlorobium phaeovibrioids* with gas vesicles. *Microbiol. Resour. Announc.* **8**(29), e00711–e719 (2019).
49. Guan, J. *et al.* Diversity and distribution of sulfate-reducing bacteria in four petroleum reservoirs detected by using 16S rRNA and *dsrAB* genes. *Int. Biodeter. Biodegr.* **76**, 58–66 (2013).
50. Nagkirti, P. D., Engineer, A. S. & Dhakephalkar, P. K. *Xylanimonas oleitrophica* sp. nov., a novel petroleum hydrocarbon degrading bacterium isolated from an Indian oil reservoir. *Anton. Leeuw. Int. J. G.* **114**, 129–136 (2021).
51. Rathi, R. *et al.* Evaluating indigenous diversity and its potential for microbial methane generation from thermogenic coal bed methane reservoir. *Fuel* **250**, 362–372 (2019).
52. Zhou, L. *et al.* Functional microorganisms involved in the sulfur and nitrogen metabolism in production water from a high-temperature offshore petroleum reservoir. *Int. Biodeter. Biodegr.* **154**, 105057 (2020).
53. Cheng, F., Jolivet, M., Guo, Z. J., Zhang, C. H. & Li, X. Z. Cenozoic evolution of the Qaidam basin and implications for the growth of the northern Tibetan plateau: A review. *Earth-Sci. Rev.* **220**, 103730 (2021).
54. Li, G. X. *et al.* Geological characteristics, evaluation criteria and discovery significance of Paleogene Yingxiongling shale oil in Qaidam Basin, NW China. *Petrol. Explor. Dev.* **49**(1), 21–36 (2022a).
55. Sun, Y., Li, Y. L., Li, L. & He, H. P. Preservation of cyanobacterial UVR-shielding pigment scytonemin in carbonate ooids formed in Pleistocene salt lakes in the Qaidam Basin, Tibetan Plateau. *Geophys. Res. Lett.* **46**(17–18), 1–28 (2019).
56. Ma, D. D. *et al.* Reservoir formation conditions and key exploration & development technologies in the Yingdong Oilfield in western Qaidam Basin. *Petrol. Res.* **3**(2), 132–151 (2018).
57. Qiao, J. Q. *et al.* Climatic and environmental conditions during the Pleistocene in the Central Qaidam Basin, NE Tibetan Plateau: Evidence from GDGTs, stable isotopes and major and trace elements of the Qiqequan Formation. *Int. J. Coal Geol.* **254**, 103958 (2022).
58. Zhuang, G. S., Hourigan, J. K., Ritts, B. D. & Kent-Corson, M. L. Cenozoic multiple-phase tectonic evolution of the northern Tibetan Plateau: Constraints from sedimentary records from Qaidam Basin, Hexi Corridor, and Subei Basin, northwest China. *Am. J. Sci.* **311**(2), 116–152 (2011).
59. Zeng, X. *et al.* Cenozoic structural characteristics and petroleum geological significance of the Qaidam Basin. *Energ. Explor. Exploit.* <https://doi.org/10.1177/01445987231152952> (2023).
60. Huang, C. G. *et al.* Characteristics, origin, and role of salt minerals in the process of hydrocarbon accumulation in the saline lacustrine basin of the Yingxi Area, Qaidam, China. *Carbonate Evaporite* **33**, 431–446 (2018).
61. Guo, Z. Q. *et al.* Main factors controlling thermogenic gas accumulation in the Qaidam Basin of western China. *Energ. Fuel.* **34**(4), 4017–4030 (2020).
62. Wu, H. *et al.* Mixed carbonate-siliciclastic reservoir characterization and hydrocarbon accumulation process of the Ganchaigou area in the western Qaidam Basin, Tibet Plateau. *Carbonate Evaporite* **37**(2), 26 (2022).
63. Guo, Z. Q. *et al.* Main factors controlling the formation of basement hydrocarbon reservoirs in the Qaidam Basin, western China. *J. Pet. Sci. Eng.* **149**, 244–255 (2017).
64. Fu, S. T., Ma, D. D., Guo, Z. J. & Cheng, F. Strike-slip superimposed Qaidam Basin and its control on oil and gas accumulation, NW China. *Petrol. Explor. Dev.* **42**(6), 778–789 (2015).
65. Wang, Y. Q. *et al.* Genesis of lacustrine carbonate breccia and its significance for hydrocarbon exploration in Yingxi region, Qaidam Basin, NW China. *Petrol. Explor. Dev.* **46**(1), 104–112 (2019).
66. Ma, X. M., Huang, C. G. & Shi, Y. J. Oil and gas enrichment patterns and major controlling factors for stable and high production of tight lacustrine carbonate rocks, a case study of Yingxi area in Qaidam Basin, West China. *Carbonate Evaporite* **34**(4), 1815–1831 (2019).
67. Xia, Q. S., Huang, C. G., Cui, J. & Li, Y. F. Reservoir space type and storage capacity of Oligocene lacustrine carbonate in the Yingxi area of western Qaidam Basin, China. *Carbonate Evaporite* **34**, 1077–1094 (2019).
68. Sun, P. *et al.* Accumulation mechanism of the Yingdong I field in the Qaidam Basin, NW China. *Petrol. Explor. Dev.* **40**(4), 461–468 (2013).
69. Wen, C. *et al.* Evaluation of the reproducibility of amplicon sequencing with Illumina MiSeq platform. *PLoS ONE* **12**, e0176716 (2017).
70. Caporaso, J. G. *et al.* Global patterns of 16S rRNA diversity at a depth of millions of sequences per sample. *Proc. Natl. Acad. Sci. U S A* **108 Suppl 1**, 4516–4522 (2011).
71. Bao, Y. P., Jin, X. H., Guo, C. L., Lu, G. N. & Dang, Z. Sulfate-reducing bacterial community shifts in response to acid mine drainage in the sediment of the Hengshi watershed, South China. *Environ. Sci. Pollut. Res.* **28**, 2822–2834 (2021).

72. Edgar, R. C., Haas, B. J., Clemente, J. C., Quince, C. & Knight, R. UCHIME improves sensitivity and speed of chimera detection. *Bioinformatics (oxford, England)* **27**, 2194–2200 (2011).
73. Li, L., Wan, Y. Y., Mu, H. M., Shi, S. B. & Chen, J. F. Interaction between illite and a *Pseudomonas stutzeri*-heavy oil biodegradation complex. *Microorganisms* **11**(2), 330 (2023b).
74. Quast, C. *et al.* The SILVA ribosomal RNA gene database project: improved data processing and web-based tools. *Nucleic Acids Res.* **41**, D590–D596 (2013).
75. Chu, X. L., Zhao, R. & Zang, W. X. Extraction of various forms of sulfur and preparation of isotopic samples from coal and sedimentary rocks. *Chin. Sci. Bull.* **38**(20), 1–4 (1993) (In Chinese).
76. Chen, K. F. *et al.* Geochemical characteristics of natural gas and hydrocarbon charge history in the western Qaidam Basin, northwest China. *Geofluids* **2020**, 2954758 (2020b).
77. Chamkha, M., Mnif, S. & Sayadi, S. Isolation of a thermophilic and halophilic tyrosol-degrading *Geobacillus* from a Tunisian high-temperature oil field. *FEMS Microbiol. Lett.* **283**(1), 23–29 (2008).
78. Czarny, J. *et al.* *Acinebacter* sp. as the key player in diesel oil degrading community exposed to PAHs and heavy metals. *J. Hazard. Mater.* **383**, 121168 (2020).
79. De Jong, S. I. *et al.* Genomic analysis of *Caldalkalibacillus thermanum* TA2.A1 reveals aerobic alkaliphilic metabolism and evolutionary hallmarks linking alkaliphilic bacteria and plant life. *Extremophiles* **24**(6), 923–935 (2020).
80. Ma, M. *et al.* Biodiversity and oil degradation capacity of oil-degrading bacteria isolated from deep-sea hydrothermal sediments of the South Mid-Atlantic Ridge. *Mar. Pollut. Bull.* **171**, 112770 (2021).
81. Dahal, R. H. & Kim, J. *Microvirga soli* sp. nov., an alphaproteobacterium isolated from soil. *Int. J. Syst. Evol. Micr.* **67**(1), 127–132 (2017).
82. Brown, S. D. *et al.* Complete genome sequence of the haloalkaliphilic, hydrogen-producing bacterium *Halanaerobium hydrogeniformans*. *J. Bacteriol.* **193**(4), 3682–3683 (2011).
83. Holochová, P. *et al.* Description of *Massilia rubra* sp. nov., *Massilia aquatica* sp. nov., *Massilia frigida* sp. nov., and one *Massilia* genomospecies isolated from Antarctic streams, lakes and regoliths. *Syst. Appl. Microbiol.* **43**(5), 126112 (2020).
84. Jiang, X. W. *et al.* Genetic and biochemical analyses of chlorobenzene degradation gene clusters in *Pandoraea* sp. Strain MCB032. *Arch. Microbiol.* **191**, 485–492 (2009).
85. Kulichevskaya, I. S., Suzina, N. E., Rijpstra, W. I. C., Damste, J. S. S. & Dedysch, S. N. *Paludibaculum fermentans* gen. nov., sp. nov., a facultative anaerobe capable of dissimilatory iron reduction from subdivision 3 of the Acidobacteria. *Int. J. Syst. Evol. Microbiol.* **64**(8), 2857–2864 (2014).
86. Nataro, J. P., Bopp, C. A., Fields, P. I., Kaper, J. B. & Strockbine, N. A. *Escherichia*, *Shigella*, and *Salmonella*. *Manual of Clinical Microbiology* 603–626 (2011).
87. Li, W. *et al.* Microbial community characteristics of petroleum reservoir production water amended with n-alkanes and incubated under nitrate-sulfate-reducing and methanogenic conditions. *Int. Biodeter. Biodegr.* **69**, 87–96 (2012).
88. Okoro, C. C. & Amund, O. O. Microbial community structure of a low sulfate oil producing facility indicate dominance of oil degrading/nitrate reducing bacteria and Methanogens. *Petrol. Sci. Technol.* **36**(4), 293–301 (2018).
89. Zhou, Z. C. *et al.* Identifying the core bacterial microbiome of hydrocarbon degradation and a shift of dominant methanogenesis pathways in the oil and aqueous phases of petroleum reservoirs of different temperatures from China. *Biogeoscience* **16**(21), 4229–4241 (2019).
90. Chen, J. L. *et al.* Changes of porcine gut microbiota in response to dietary chlorogenic acid supplementation. *Appl. Microbiol. Biot.* **103**, 8157–8168 (2019a).
91. Zhou, L. *et al.* Dominant and active methanogens in the production waters from a high-temperature petroleum reservoir by DNA- and RNA-based analysis. *Geomicrobiol. J.* **38**(3), 1822958 (2021).
92. Liang, B. *et al.* High frequency of *Thermodesulfovibrio* spp. and Anaerolineaceae in association with *Methanoculleus* spp. In a long-term incubation of n-alkanes-degrading methanogenic enrichment culture. *Front. Microbiol.* **7**, 1431 (2016).
93. Vick, S. H. W., Greenfield, P., Tetu, S. G., Midgley, D. J. & Paulsen, I. T. Draft genome sequence of *Dietzia* sp. Strain SYD-A1, isolated from coal seam formation water. *Microbiol. Resour. Ann.* **10**(10), e01341-20 (2021).
94. Jadav, S., Sakthipriya, N., Doble, M. & Sangwai, J. S. Effect of biosurfactants produced by *Bacillus subtilis* and *Pseudomonas aeruginosa* on the formation kinetics of methane hydrates. *J. Nat. Gas Sci. Eng.* **43**, 156–166 (2017).
95. Dastgheib, S. M. M., Amoozegar, M. A., Elahi, E., Asad, S. & Banat, I. M. Bioemulsifier production by a halothermophilic *Bacillus* strain with potential applications in microbially enhanced oil recovery. *Biotechnol. Lett.* **30**, 263–270 (2008).
96. Choudhury, S. P., Panda, S., Haq, I. & Kalamdhad, A. S. Enhanced methane production and hydrocarbon removal from petroleum refinery sludge after *Pseudomonas putida* pretreatment and process scale-up. *Bioresour. Technol.* **343**, 126127 (2022).
97. Allegue, T., Arias, A., Fernandez-Gonzalez, N., Omil, F. & Garrido, J. M. Enrichment of nitrite-dependent anaerobic methane oxidizing bacteria in a membrane bioreactor. *Chem. Eng. J.* **347**, 721–730 (2018).
98. Martins, P. D. *et al.* Sulfide toxicity as key control on anaerobic oxidation of methane in eutrophic coastal sediments. *BioRxiv* **2022-02**, 479873 (2022).
99. Šantl-Temkiv, T., Finster, K., Hansen, B. M., Pašić, L. & Karlson, U. G. Viable methanotrophic bacteria enriched from air and rain can oxidize methane at cloud-like conditions. *Aerobiologia* **29**(3), 373–384 (2013).
100. Yang, H., Jung, H., Oh, K., Jeoh, J. M. & Cho, K. S. Characterization of the bacterial community associated with methane and odor in a pilot-scale landfill biocover under moderately thermophilic conditions. *J. Microbiol. Biotechnol.* **31**(6), 803–814 (2021).
101. Zuniga, C., Morales, M., Le Borgne, S. & Revah, S. Production of poly-beta-hydroxybutyrate (PHB) by methylobacterium organophilum isolated from a methanotrophic consortium in a two-phase partition bioreactor. *J. Hazard. Mater.* **190**(1–3), 876–882 (2011).
102. Abdallah, M. B. *et al.* Prokaryotic diversity in a Tunisian hypersaline lake, Chott El Jerid. *Extremophiles* **20**, 125–138 (2016).
103. Li, X. *et al.* The bioenergetics mechanisms and applications of sulfate-reducing bacteria in remediation of pollutants in drainage: A review. *Ecotoxicol. Environ. Saf.* **158**, 162–170 (2018).
104. Thiel, V. *et al.* “Candidatus Thermomonobacter thiotrophicus”, a non-phototrophic member of the Bacteroidetes/Chlorobi with dissimilatory sulfur metabolism in hot spring mat communities. *Front. Microbiol.* **9**, 3159 (2019).
105. Liang, C. L. *et al.* Sediment pH, not the bacterial diversity, determines *Escherichia coli* O157:H7 survival in estuarine sediments. *Environ. Pollut.* **252**, 1078–1086 (2019).
106. Lahme, S. *et al.* Metabolites of and oil field sulfide-oxidizing, nitrate-reducing *Sulfurimonas* sp. cause severe corrosion. *Appl. Environ. Microbiol.* **85**(3), 01891–18 (2019).
107. Koenig, A., Zhang, T., Liu, L. H. & Fang, H. H. P. Microbial community and biochemistry process in auto sulfurotrophic denitrifying biofilm. *Chemosphere* **58**(8), 1041–1047 (2005).
108. Jing, C., Ping, Z. & Mahmood, A. Influence of various nitrogenous electron acceptors on the anaerobic sulfide oxidation. *Bioresour. Technol.* **101**(9), 2931–2937 (2010).
109. Liu, Z. G. *et al.* Mixed carbonate rocks lithofacies features and reservoirs controlling mechanisms in a saline lacustrine basin in Yingxi area, Qaidam Basin, NW China. *Petrol. Explor. Dev.* **48**(1), 80–94 (2021).
110. Dulger, S., Demirbag, A. & Belduz, A. S. *Anoxybacillus ayderensis* sp. nov. and *Anoxybacillus kestanbolensis* sp. nov.. *Int. J. Syst. Evol. Micr.* **54**(5), 1499–1503 (2004).

111. Kadnikov, V. V., Mardanov, A. V., Beletsky, A. V., Karnachuk, O. V. & Ravin, N. V. Microbial life in the deep subsurface aquifer illuminated by metagenomics. *Front. Microbiol.* **11**, 572252 (2020).
112. Park, H., Brotto, A. C., Van Loosdrecht, M. C. M. & Chandran, K. Discovery and metagenomic analysis of an anammox bacterial enrichment related to *Candidatus "Brocadia caroliniensis"* in a full-scale glycerol-fed nitritation-denitritation separate centrate treatment process. *Water Res.* **111**, 265–273 (2017).
113. Dalsing, B., Truchon, A. N., Gonzalez-Orta, E. T., Milling, A. S. & Allen, C. *Ralstonia solanacearum* uses inorganic nitrogen metabolism for virulence, ATP production, and detoxification in the oxygen-limited host xylem environment. *MBio* **6**(2), 1–13 (2015).
114. Yin, X. Y., Rahaman, M. H., Liu, W. B., Makinia, J. & Zhai, J. Comparison of nitrogen and VFA removal pathways in autotrophic and organotrophic anammox reactors. *Environ. Res.* **197**, 111065 (2021).
115. Tapia-García, E. Y. *et al.* *Paraburkholderia lycopersici* sp. nov., a nitrogen-fixing species isolated from rhizoplane of *Lycopersicon esculentum* Mill. var. *Saladette* in Mexico. *Syst. Appl. Microbiol.* **43**(6), 126133 (2020).
116. Gao, Y., Dai, L. K., Zhu, H. D., Chen, Y. L. & Zhou, L. Quantitative analysis of main components of natural gas based on Raman Spectroscopy. *Chin. J. Anal. Chem.* **47**(1), 67–76 (2019).
117. Wang, X. F. *et al.* Hydrogen isotope characteristics of thermogenic methane in Chinese sedimentary basins. *Org. Geochem.* **83–84**, 178–189 (2015).
118. Zhang, S. C. *et al.* Unique chemical and isotopic characteristics and origins of natural gases in the Paleozoic marine formations in the Sichuan Basin, SW China: Isotope fractionation of deep and high mature carbonate reservoir gases. *Mar. Petrol. Geol.* **89**, 68–82 (2018).
119. Han, W. X. *et al.* Carbon isotope reversal and its relationship with natural gas origins in the Jingbian gas field, Ordos Basin, China. *Int. J. Coal Geol.* **196**, 260–273 (2018).
120. Liu, Q. Y. *et al.* Carbon and hydrogen isotopes of methane, ethane, and propane: A review of genetic identification of natural gas. *Earth-Sci. Rev.* **190**, 247–272 (2019).
121. Song, C. P. Hydrogen isotopic characteristics, origin of natural gas and gas-source correlation in the Qaidam Basin. 1–100 (Master Thesis, University of Chinese Academy of Sciences, Beijing, 2006) (In Chinese).
122. Zhang, X. B. *et al.* The characteristics, origination and distribution of carbon isotope in the Paleocene saline lacustrine natural gas from western Qaidam Basin. *Sci. China Ser. D* **32**(7), 598–608 (2003) (In Chinese).
123. Zhang, Y. S. *et al.* Genesis, type and reservoir formation law of natural gas in western Qaidam Basin. *China Pet. Explor.* **24**(4), 1–11 (2019).
124. Zhao, D. S. *et al.* Characteristics of carbon isotope and origin of natural gas in Qaidam Basin. *Acta Sedimentol. Sin.* **24**(01), 135 (2006) (In Chinese).
125. Feng, Z. Q. *et al.* Shale gas geochemistry in the Sichuan Basin. *China. Earth-Sci. Rev.* **232**, 104141 (2022).
126. Liu, C. L. *et al.* Geochemical features of natural gas in the Qaidam Basin. *NW China. J. Pet. Sci. Eng.* **110**, 85–93 (2013).
127. Li, J. *et al.* Geochemical characteristics and source analysis of natural gas in the saline lacustrine basin in the Western Qaidam basin. *J. Pet. Sci. Eng.* **201**, 108363 (2021b).
128. Ni, Y. Y. *et al.* Geochemical characteristics of biogenic gases in China. *Int. J. Coal Geol.* **113**, 76–87 (2013).
129. Ni, Y. Y. *et al.* Hydrogen isotopes of hydrocarbon gases from different organic facies of the Zhongba gas field, Sichuan Basin, China. *J. Pet. Sci. Eng.* **179**, 776–786 (2019).
130. Shuai, Y. H. *et al.* Microbial consortia controlling biogenic gas formation in the Qaidam Basin of western China. *J. Geophys. Res.-Biogeo.* **121**(8), 2296–2309 (2016).
131. Zhang, S. C., Mi, J. K. & He, K. Synthesis of hydrocarbon gases from four different carbon sources and hydrogen gas using a gold-tube system by Fischer-Tropsch method. *Chem. Geol.* **349–350**, 27–35 (2013).
132. Whiticr, M. J. Carbon and hydrogen isotope systematics of bacterial formation and oxidation of methane. *Chem. Geol.* **161**(1–3), 291–314 (1999).
133. Chen, G. *et al.* Anomalous positive pyrite sulfur isotope in lacustrine black shale of the Yanchang formation, Ordos Basin: Triggered by paleoredox chemistry changes. *Mar. Petrol. Geol.* **121**, 104587 (2020a).
134. Xiao, Q. L., Cai, S. Y. & Liu, J. Z. Microbial and thermogenic hydrogen sulfide in the Qianjiang Depression of Jiangnan Basin: Insights from sulfur isotope and volatile organic sulfur compounds measurements. *Appl. Geochem.* **126**, 104865 (2021).
135. Li, P. P. *et al.* Sulfate sources of thermochemical sulfate reduction and hydrogen sulfide distributions in the Permian Changxing and Triassic Feixianguan formations, Sichuan Basin, SW China. *Mar. Petrol. Geol.* **145**, 105892 (2022b).
136. Kong, X. X. *et al.* Fine-grained carbonate formation and organic matter enrichment in an Eocene saline rift lake (Qianjiang Depression): Constraints from depositional environment and material source. *Mar. Petrol. Geol.* **138**, 105534 (2022).
137. Zhu, G. Y. *et al.* Induced H₂S formation during steam injection recovery process of heavy oil from the Liaohe Basin, NE China. *J. Pet. Sci. Eng.* **71**(1–2), 30–36 (2010).

Acknowledgements

We gratefully thank Jijun Li, Yizhe Wang, Xutong Guan and Cong Lin for field assistance in the southwestern Qaidam Basin. We are also indebted to Yong Nie, Lilei Liu, Jianwei Wang, Huajian Wang, Changfu Fan for their assistance with pretreatment and measurement of samples. We are grateful to proof-readers and editors. This work was supported by the National Natural Science Foundation of China [grant numbers 42072125].

Author contributions

Y.J.: Conceptualization, formal analysis, writing-original draft, methodology. L.A.: Methodology, investigation, formal analysis, data curation. W.W.: Resources, investigation, funding acquisition. J.M.: Methodology, writing-original draft, formal analysis, visualization. C.W.: Conceptualization, methodology, visualization, supervision, funding acquisition. X.W.: Conceptualization, methodology, supervision, funding acquisition.

Competing interests

The authors declare no competing interests.

Additional information

Supplementary Information The online version contains supplementary material available at <https://doi.org/10.1038/s41598-023-33978-3>.

Correspondence and requests for materials should be addressed to C.W.

Reprints and permissions information is available at www.nature.com/reprints.

Publisher's note Springer Nature remains neutral with regard to jurisdictional claims in published maps and institutional affiliations.



Open Access This article is licensed under a Creative Commons Attribution 4.0 International License, which permits use, sharing, adaptation, distribution and reproduction in any medium or format, as long as you give appropriate credit to the original author(s) and the source, provide a link to the Creative Commons licence, and indicate if changes were made. The images or other third party material in this article are included in the article's Creative Commons licence, unless indicated otherwise in a credit line to the material. If material is not included in the article's Creative Commons licence and your intended use is not permitted by statutory regulation or exceeds the permitted use, you will need to obtain permission directly from the copyright holder. To view a copy of this licence, visit <http://creativecommons.org/licenses/by/4.0/>.

© The Author(s) 2023